International Journal of Energy
ISSN: 2957-9473 | Vol. 9, No. 2, 2026

Research on the Dynamic Regulation of Bacterial Contaminated Particulate Matter in Operating Rooms Using Turbulent Jet Devices

Beibei Wang, Yue Feng, Yiting Wang, Zhenying Zhang and Meiyuan Yang

North China University of Science and Technology, Tangshan, Hebei, 063210, China

Abstract: As the core operational venue in the healthcare system, the precise control of environmental parameters in operating rooms is crucial for ensuring surgical safety and reducing healthcare-associated infection risks. The rational airflow organization serves as the key mechanism for achieving refined environmental regulation in operating rooms. With continuously rising demands for surgical environments driven by advancements in medical technology, traditional airflow management methods have increasingly revealed limitations such as uneven temperature distribution and low pollutant removal efficiency, necessitating the introduction of novel technological solutions for optimization. The vortex-breaking jet device, leveraging its technical advantages in fluid vortex control, offers innovative approaches for optimizing operating room airflow. This study investigates the application of vortex-breaking jet devices in operating room airflow management, aiming to elucidate their mechanisms of influence on the surgical environment and provide a theoretical foundation for the design and optimization of operating room airflow systems.

Keywords: Heat and Mass Transfer; Airflow Organization; Clean Operating Room; Vortex-breaking Jet Device.

1. Introduction

The operating room, as the core venue for emergency rescue and life-saving procedures, has its environmental quality directly determining the success rate of surgeries and the postoperative recovery process of patients. Unlike general ward environments, the operating room must simultaneously maintain constant temperature and humidity under steady-state conditions while ensuring precise control of bacterial concentration. The fulfillment of these specialized requirements fundamentally relies on the dynamic regulation of the surgical environment through airflow organization via heat and mass transfer processes. Airflow serves not only as a carrier of heat and humidity but also as a "transport channel" for pollutant migration. Its flow pattern, velocity distribution, and diffusion pathways directly determine the cleanliness, thermal comfort, and stability of the intraoperative microenvironment.

A vortex-breaking jet device is a system that disrupts or mitigates vortex formation and development in fluid flows by injecting jet streams. It has been widely implemented in deep-sea mining, hydropower plants, and industrial fluid systems. When integrated with air inlets, this device eliminates pollutant accumulation caused by localized vortices while directing clean airflow to target areas and forcing contaminated air toward exhaust outlets, thereby enhancing air displacement efficiency.

This paper focuses on investigating the heat and mass transfer processes in operating room airflow organization facilitated by vortex-breaking jet systems. First, it outlines the specific requirements of the operating room environment for heat and mass transfer and clarifies the correlation between airflow parameters and environmental quality indicators. Second, it analyzes the heat and mass transfer efficiency of laminar flow and elucidates the coupling patterns between the airflow field, temperature field, and pollutant concentration field under dynamic operating conditions. Finally, based on the research findings, the paper proposes technical approaches for optimizing airflow organization design and develops air conditioning systems compliant with clean operating room standards, providing theoretical support and practical guidance for improving operating room environmental quality and reducing surgical complication rates.

2. Research on the 2-layer Laminar Air Supply System for Clean Environment Applications

2.1. Current Status and Progress

As the core technology ensuring air quality in high-cleanliness environments such as operating rooms and electronic workshops, laminar airflow delivery technology has garnered significant attention for its performance optimization research. This article systematically reviews recent advancements in laminar airflow delivery systems, with a focus on analyzing the influencing factors and technical research methodologies.

2.2. Analysis of Influencing Factors

The air quality in operating rooms is crucial for controlling surgical wound infections and even postoperative hospital-acquired infections [1]. The gold standard for evaluating operating room air quality is bacterial load, as airborne bacteria primarily adhere to particles and disseminate through the air via these particles [2]. During dispersion, particle trajectories are influenced by multiple factors, including airflow parameters, indoor heat sources, and building envelope characteristics. Based on the operational characteristics of each clean operating room and the interpretation of relevant standards, the air conditioning system should employ a centralized fresh air system to eliminate the wet load within the operating room, while a recirculating air conditioning system regulates indoor

temperature. These two systems independently control temperature and humidity, ensuring the entire clean operating area remains under controlled conditions and allowing flexible utilization of individual operating rooms [3].

2.2.1. Influence of Airflow Parameters

Wind speed: As a core control parameter for laminar flow, there exists an optimal range. Li Xiaolei, Ni Ming, et al. demonstrated through clinical experiments that in ISO Class 5 operating rooms, increasing the vertical laminar flow velocity from 0.2 m/s to 0.3 m/s resulted in a significant reduction of airborne bacterial concentration in the surgical area by approximately 24%-32% [4]. However, this improvement is not linear. CFD simulations of wind speed gradients conducted by Gao Qing, Liu Ringshuai, et al. revealed that when the wind speed exceeds 0.35 m/s, the decline in bacterial concentration slows down (<10%), while turbulent disturbances increase instead [5].

Air supply temperature and uniformity: Haiyi Du et al. (2024) found through multi-point temperature sensing measurements that air supply temperature uniformity is critical for preventing vertical temperature stratification. When the temperature difference at supply outlets exceeds 0.5°C, a horizontal temperature difference of over 1°C may occur in the work area, compromising thermal comfort [6]. Zhang Zechao et al. (2021) emphasized that air supply temperature settings must account for surgeons' heat load (approximately 100–150 W), as excessively low temperatures accelerate airflow updrafts and generate vortices [7].

Air supply angle: A slight angle setting controls particle trajectory.

2.2.2. Impact of Indoor Heat Sources

Thermal effect of surgical lamps: Shadowless lamps serve as significant interference sources. The localized photothermal radiation and temperature elevation generated during illumination primarily stem from the infrared components of the light source and energy loss conversion. This can lead to tissue drying and localized overheating in the surgical field, increasing the risk of intraoperative thermal injury, and adversely affecting the thermal environment of the operating room and patient body temperature regulation.

Medical staff activities and metabolic heat: The density of human heat sources (approximately 80–120 W per person) influences airflow organization. Zhou Weiming et al. (2024) observed in a scaled-down laboratory simulating a surgical environment that adding one medical staff member increases the air age in the head region by approximately 18 seconds compared to a single personnel, disrupting pollutant removal pathways [8]. Bian Jinlong et al. (2023) conducted field measurements using tracer gases on human models and found that changes in the standing positions of medical staff can cause pollutant concentration fluctuations in the surgical area exceeding 30% [9].

Analysis of Equipment Heat Source Impact: Guo et al. (2022) recommend addressing dynamic heat source disturbances through optimized equipment layout combined with variable air volume (VAV) control [10].

2.2.3. Effects of the Envelope Structure

Wall insulation performance: When the exterior wall temperature approaches the indoor temperature, heat exchange is minimized. Ankang Kan et al. (2017) empirically compared the performance of walls with different insulation materials: Walls equipped with vacuum insulation panels (VIP) increased the interior wall temperature by approximately 1.8°C in summer compared to conventional walls (approaching room temperature), effectively reducing the natural convection heat flux by nearly 60% (from about 3.7 W/m² to 1.5 W/m²) and mitigating the interference of cold wall-induced airflow on the main supply airflow [11]. This corroborates the "thermal compensation interior wall design" concept proposed by Alamdari et al. (2017) [12].

Design of return air outlet position and dimensions: The layout of air outlets directly affects the return flow ratio. Guo Peishan et al. (2020) investigated the uniformity of the airflow field under different air outlet aspect ratios and found that when the aspect ratio is <0.6, the uniformity index (UI) of the core zone airflow exceeds 0.98; however, when the aspect ratio is too high (>0.8), the UI drops to 0.91, leading to vortex formation [13].

Impact of Air Infiltration and Air Tightness: Door and window leakage is one of the causes of cleanliness deterioration. The European standard EN ISO 14644-3:2019 explicitly specifies the air tightness requirements for building envelopes (air change rate <0.2 h^{-1} under a pressure differential of 50 Pa) [14]. Du Shiyuan et al. (2007) quantitatively analyzed the impact of insufficient air tightness (defined as a gap area ratio of 0.5%) on clean areas; upon door opening, external contaminants can infiltrate, causing a temporary drop in the local ISO cleanliness level to grades 6–7 [15].

3. Vortex-jet Device

Based on the vortex-breaking principle for air purification, the device's air inlets or flow-guiding components typically feature guide vanes, spiral channels, or porous straightening structures. As airflow passes through, these structures break down the readily generated chaotic turbulence and wall-mounted vortices into multiple directional fine jets. By adjusting the jet angles and outlet velocity, the multiple jets superimpose and merge within the space, creating a uniform velocity field. This approach not only eliminates pollutant retention caused by localized vortices but also directs the clean airflow to cover the target area while forcing contaminated air toward the exhaust outlet, thereby enhancing air exchange efficiency.

3.1. Current Application Scope

In deep-sea mining applications, this device prevents pipeline blockages in mineral slurry conveyance by controlling fluid vortices; during hydropower station operations, it optimizes water flow fields to enhance turbine generator efficiency, fully demonstrating the technical advantages of fluid intervention and vortex control. When integrated into operating room airflow systems, the device actively mitigates vortex formation, addressing limitations of conventional airflow configurations. This technological adaptation not only expands the application scope of vortex-breaking jet devices but also provides innovative solutions for operating room environmental control, holding significant practical value. However, research on applying vortex-breaking jet devices to building indoor environmental control—particularly in specialized clean spaces like operating rooms—remains limited. Existing literature primarily focuses on conceptual discussions or basic flow field simulations, lacking systematic design methodologies or engineering implementation cases.

3.2. Optimization of the Air Supply System for the Vortex Jet Device

In the airflow organization of operating rooms, the core function of the vortex-breaking jet device is to enhance the uniformity of air supply jet distribution, suppress indoor vortex formation, and improve cleanliness maintenance capability. Its specific application focuses on optimizing the air supply system in clean operating rooms.

3.2.1. Optimizing Laminar Air Supply Performance

In traditional clean operating rooms, laminar airflow often generates localized vortexes beneath the ceiling and around the operating table, leading to pollutant retention. By integrating vortex-breaking jet devices at the air supply outlets of high-efficiency filters, the directional jet characteristics of these devices can "disperse" the wall-adhesion effect and vortex zones of the supplied airflow. This enables more uniform vertical downward airflow distribution, creating a stable clean air curtain that covers the operating table and aseptic work areas, thereby reducing the likelihood of surgical site contamination by surrounding air.

3.2.2. Airflow Pattern in the Control Room

For the airflow organization requirements of different levels of clean operating rooms (e.g., Level I orthopedic implantation surgeries and Level II general surgical procedures), the diffusion range and deceleration rate of airflow can be precisely controlled by adjusting the jet angle and outlet air velocity of the vortex-breaking jet device.

3.2.3. Suppression of Turbulence Effects on Personnel and Equipment

The movement of medical staff and the arrangement of surgical instrument tables in the operating room can disrupt the original laminar airflow, creating localized turbulence. Small vortex-breaking jet outlets can be installed in peripheral areas of the operating room (e.g., above instrument tables and beside personnel pathways). These lateral auxiliary jets counteract the disturbances generated by personnel movement, maintaining stable airflow in the core surgical zone and minimizing the dispersion of contaminants into the surgical area.

3.2.4. Enhancing Displacement Efficiency Through Coordinated Ventilation System

The vortex-guided jet device directs clean airflow toward the surgical room's exhaust vents, creating an efficient "top supply, bottom exhaust" air exchange pattern. This facilitates rapid removal of microbial-laden air and anesthetic byproducts, prevents pollutant retention and circulation within the room, and reduces the risk of cross-contamination between different areas.

4. Analysis of Technical Research Methods

This experiment utilized the ANSYS simulation software to establish a operating room model, analyzing heat and mass transfer within the enclosed operating room. The air supply outlet was positioned directly above the operating table, with two return air outlets of identical specifications installed on both sides below. The study compared airflow patterns before and after integrating the air supply outlet with a vortex-breaking jet device, selecting the optimal ventilation configuration to ensure a clean indoor environment, reduce wound infection rates, and establish a sterile operating room.

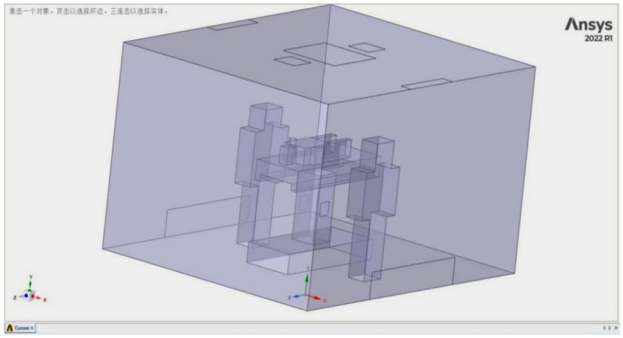

Figure 1. 3D model of a clean operating room

Table 1. Data Parameters of Clean Operating Rooms

name	Number (units)	size (m)	remarks
operating room	1	5*4	
Air Inlet 1	1	1*1	
Air Inlet 2	2	0.4*0.4	Wind curtain (located on the ceiling)
Air Inlet 3	2	0.2*0.2	Turbulent Jet Device (Located on both sides of the operating table)
Exhaust vent 1	2	1*0.4	On both sides
Exhaust vent 2	2	1*0.2	On the ceiling
staff	2	1.8*0.3	
patient	1	1.8*0.4	
operating table	1	2*0.5*1	

By comparing the presence and absence of vortex-breaking jet devices, this study investigates the impact of such devices on airflow organization in clean operating rooms.

The function of the airflow distribution cloud map: Intuitively displays the distribution of indoor wind speed, temperature, pressure, and pollutant concentration; rapidly identifies airflow dead zones, vortices, temperature gradients, and short-circuiting issues; evaluates the effectiveness of ventilation, air conditioning, and cleanroom airflow; guides the optimization of air outlets, airflow volume, and layout to enhance comfort and energy efficiency.

The airflow distribution maps in Figures 2, 3, and 4 clearly demonstrate that the addition of vortex-breaking jet devices in the clean operating room reduces the vortices beneath the operating table and adjacent to the air intake, enhances airflow efficiency, suppresses the secondary circulation and retention of contaminated gases, and thereby improves the cleanliness and comfort within the operating room.

4.1. Advances in Numerical Simulation Research

The pivotal role of CFD in airflow modeling: Cen Dongdong et al. (2018) employed ANSYS Fluent to numerically reconstruct the non-isothermal flow field in a real operating room (using the RNG k-ε turbulence model and DO radiation model), successfully capturing the vortex structure formed by thermal plumes beneath the surgical lamp, with the temperature deviation from measured values controlled within ±0.5°C [16]. Liu Haiyang et al. (2021) utilized the Discrete Phase Model (DPM) coupled with transient flow

field analysis to investigate the impact of physician turning movements on aerosol trajectory propagation, achieving a computational efficiency approximately 300% higher than that of full-scale LES, with accuracy meeting engineering design requirements [17].

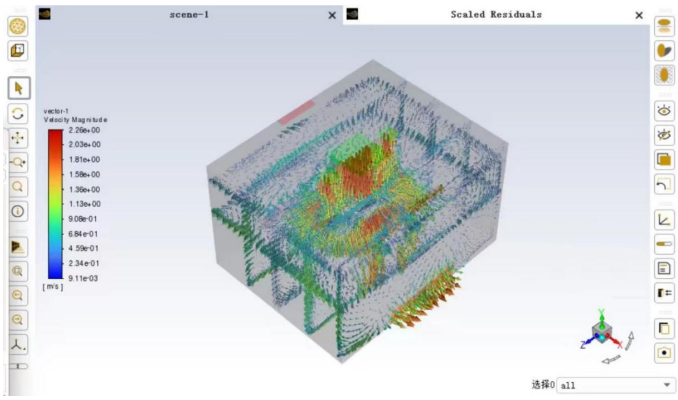

Figure 2. Cloud map of airflow organization distribution with the vortex-breaking jet device

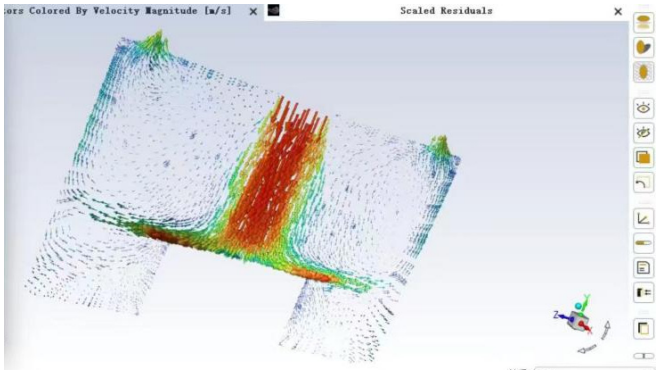

Figure 3. Cloud map of indoor airflow distribution for the vortex-free jet device (1)

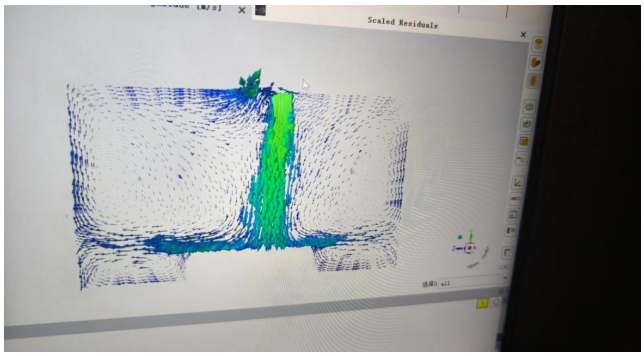

Figure 4. Cloud map of indoor airflow distribution for the vortex-free jet device (2)

Innovation in multi-physics coupled modeling: Distribution of particle mass concentration and gas concentration in the surgical area. Liu Shuanqiang, Liu Xiaohua, Jiang Yi et al. (2009) established a dynamic thermal source response mechanism by developing a user-defined function (UDF) incorporating personnel motion functions and light thermal power curves, enabling dynamic simulation under variable operating conditions [18].

4.2. Solution Calculation

4.2.1. Basic Control Equation (Core Conservation Laws of Fluid Mechanics)

The flow obeys the three laws of conservation of mass, momentum, and energy. For incompressible air (low-speed flow with Ma <0.3, where density can be approximated as constant), combined with the Reynolds averaging method, the governing equations are as follows:

(1) The mass conservation equation (continuity equation) tensor form:

$$\frac{\partial u_i}{\partial x_i} = 0$$

expansion format (3D Cartesian coordinates):

$$\frac{\partial u}{\partial x} + \frac{\partial v}{\partial y} + \frac{\partial w}{\partial z} = 0$$

These u, v, wrepresent the instantaneous velocities in the x/y/z directions, respectively. In this case, this conservation law holds true, with the total inflow flow rate equal to the total outflow flow rate.

(2) Momentum conservation equation (Reynolds averaging N-S equation)

Considering the effects of gravity and buoyancy, and incorporating the Boussinesq assumption used in this experiment (which accounts for density variations only in the buoyancy term, while treating all other terms as reference constants—a significant simplification that better models natural convection under small temperature differentials)—the equation is as follows:

$$\rho_0 \frac{\partial (u_i u_j)}{\partial x_j} = -\frac{\partial p}{\partial x_i} + \frac{\partial}{\partial x_j}\left[\mu\left(\frac{\partial u_i}{\partial x_j} + \frac{\partial u_j}{\partial x_i}\right)\right] + \frac{\partial\left(-\rho_0 \overline{u_i' u_j'}\right)}{\partial x_j} - \rho_0 g \beta (T - T_0)\delta_{iy}$$

All explanations:

$\rho_0$1.225 kg/m^{3}Reference air density, measured under standard conditions

pμg : Average static pressure: Aerodynamic viscosity: Gravitational acceleration

$-\rho_0 \overline{u_i' u_j'}$The Reynolds stress term requires closure by a turbulence model.

$\beta\beta = 1/T_0 T_0$The coefficient of thermal expansion of air, under ideal gas conditions, is used as the reference intake air temperature.

(3) The equation of energy conservation

For low-speed flow, viscous dissipation can be neglected, and the equation is simplified as follows:

$$\rho_0 c_p \frac{\partial (u_j T)}{\partial x_j} = \frac{\partial}{\partial x_j}\left(\lambda \frac{\partial T}{\partial x_j}\right)$$

Where $c_p \lambda T$c_A is the specific heat capacity of air at constant pressure, k_A is the thermal conductivity of air, and T_f is the fluid temperature.

4.2.2. Closed Equation of the RNG k-ε Turbulence Model

This case employs the RNG k-ε turbulence model, commonly used in engineering kεfluid dynamics, with the

core objective of solving the turbulent kinetic energy and dissipation rate to achieve closure of the Reynolds stress term.

(1) Turbulent kinetic transport equation k

$$\rho_0 \frac{\partial(u_j k)}{\partial x_j} = \frac{\partial}{\partial x_j}\left[\left(\mu + \frac{\mu_t}{\sigma_k}\right)\frac{\partial k}{\partial x_j}\right] + P_k + P_b - \rho_0 \varepsilon$$

(2) Dissipation rate ε transport equation

$$\rho_0 \frac{\partial(u_j \varepsilon)}{\partial x_j} = \frac{\partial}{\partial x_j}\left[\left(\mu + \frac{\mu_t}{\sigma_\varepsilon}\right)\frac{\partial \varepsilon}{\partial x_j}\right] + \frac{C_{1\varepsilon}\varepsilon}{k}(P_k + C_{3\varepsilon}P_b) - C_{2\varepsilon}\rho_0 \frac{\varepsilon^2}{k}$$

parameter declaration:

$$\text{Turbulent viscosity: } \mu_t = \rho_0 C_\mu \frac{k^2}{\varepsilon}$$

$$\text{Model default constant: } C_\mu = 0.0845, C_{1\varepsilon} = 1.42, C_{2\varepsilon} = 1.68, \sigma_k = 0.7194, \sigma_\varepsilon = 0.7194$$

$P_k P_b$For the velocity gradient turbulent kinetic energy term and the buoyancy turbulent kinetic energy term, this case involves temperature difference buoyancy, necessitating the inclusion of both terms.

4.2.3. Calculation Process of Boundary Parameters for This Case

Based on the relevant experimental data, calculate the boundary parameters required for the simulation:

(1) Basic Dimension Calculation

Room Volume:

$$V = 5\ \text{m} \times 4\ \text{m} \times 3\ \text{m} = 60\ \text{m}^3$$

Total air intake area:

$$S = 1\ \text{m} \times 1\ \text{m} + 2 \times 0.4\ \text{m} \times 0.4\text{m} + 2 \times 0.2\text{m} \times 0.2\text{m} = 1.4\ \text{m}^2$$

Total return air area:

$$S = 2 \times 1\ \text{m} \times 0.4\ \text{m} + 2 \times 1\ \text{m} \times 0.2\text{m} = 0.12\ \text{m}^2$$

(2) Calculation of Air Inlet Parameters

The standard requirements for a clean $n = 25$operating room specify an air exchange rate of [number] times per hour, with a total calculated air volume:

$$Q = \frac{nV}{3600} = \frac{25 \times 60}{3600} \approx 0.417\ \text{m}^3/\text{s}$$

According to the continuity $Q = v_{in}S_{in}$ equation, the average air intake velocity is obtained as follows:

$$v_{in} = \frac{Q}{S_{in}} = \frac{0.417}{1.4} \approx 0.3\ \text{m/s}$$

(3) Turbulence parameter calculation

Entrance turbulence is typically I characterized by turbulence intensity, with the calculation formula as follows:

$$I = 0.16\left(Re_{D_h}\right)^{-1/8}, \quad Re_{D_h} = \frac{\rho v D_h}{\mu}$$

The hydraulic diameter of $D_h = \frac{2ab}{a+b}$the rectangular air inlet is as follows: the experimental calculation yields an inlet turbulence intensity of approximately 5%, meeting the requirements for conventional engineering installations.

(4) Calculation of heat source parameters

The problem specifies a body surface temperature of 35°C for medical $T = 35°C = 308.15\ \text{K}$ personnel; setting it directly as a constant-temperature wall boundary meets the requirements. If configured as a heat flux boundary, the resting heat dissipation per individual is approximately 110 W, resulting in a total heat flux of:

$$Q_h = 2 \times 110 = 220\ \text{W}$$

4.2.4. Result Evaluation Calculation Formula

Once the flow field and temperature field results are obtained, the ventilation effectiveness can be quantitatively evaluated using the following formula:

$$\text{Average air age (a measure of air freshness; the lower the value} \tau_{avg} = \frac{1}{V}\int_V \tau\, dV, \text{the fresher the air):}$$

$$\text{Ventilation efficiency (a measure of the rationality of ventilation } \eta = \frac{V/(2Q)}{\tau_{avg}} \times 100\% \text{design; higher values indicate greater efficiency):}$$

4.2.5. Experimental Flowchart

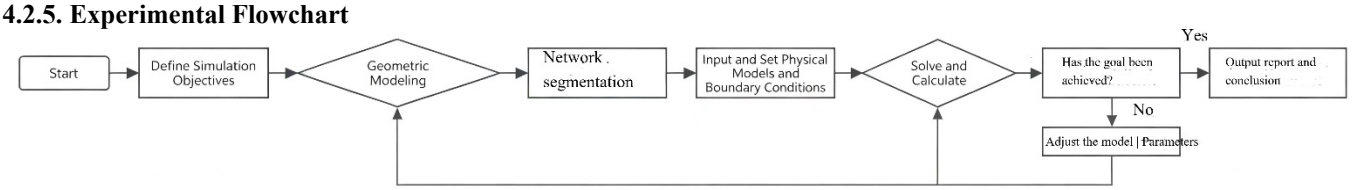

Figure 5. Flowchart

4.3. Comparison and Integration of Numerical Simulation and Experimental Testing Methods

Analysis of Complementary Methodological Advantages: A comprehensive review of existing research delineates the applicable boundaries for the two methods: CFD possesses robust three-dimensional flow field visualization capabilities, enabling preliminary screening of hundreds of operating conditions at relatively low cost [19]. Particularly under complex boundary conditions such as personnel thermal plumes, Yang Shaodong, Ding Changfu, Wang Yin, et al. (2025) found that comparing the flow field structures obtained via particle image velocimetry (PIV) with CFD simulations necessitates adjustments to turbulence model constants to improve predictions of thermal plume ascent heights (original model error of 25%, reduced to 15% after correction) [20].

The trend toward multiscale model integration: Developing a macro-micro coupled framework to enhance computational accuracy and efficiency has become a focal point. Deng Zhiyao, Lin Yaolin, Liu Naiwei, et al. (2026) proposed a zonal coupling strategy: dividing rooms into a core zone (high-resolution grid) and corner zones (coarse grid), which ensures precise flow field representation around occupants while reducing overall computation time by 45% [21].

A new data-driven modeling paradigm leveraging machine learning tools: By utilizing the heating IoT's capability to collect real-time flow and pressure measurements from heat sources and thermal stations, this approach employs a data-model fusion-driven methodology. It generates leakage fault datasets for heating networks through steady-state hydraulic

simulation models, followed by training machine learning models [22]. Tian Yushi (2015) developed an adaptive control framework based on BACnet and LonTalk, which adjusts damper openings across zones in real-time using sensor data feedback to achieve dynamic energy consumption optimization [23].

5. Existing Issues and Challenges

The operating room ventilation system serves as the core barrier for hospital infection control, and its performance is directly correlated with the incidence of surgical site infections (SSI), healthcare workers' occupational health, and hospital energy consumption levels [24]. With the advancement of precision medicine and the "dual carbon" goals, the limitations of traditional ventilation systems in terms of dynamic adaptability, multi-objective balance, and response to specialized scenarios have become increasingly apparent.

5.1. Compatibility between Practical Applications and Theoretical Simulations

As the core tool for operating room ventilation system design, CFD simulation's accuracy directly determines the effectiveness of engineering solutions; however, modeling deviations under dynamic scenarios have become a widespread challenge in the industry.

This is specifically manifested in three dimensions: First, the simplified treatment of personnel disturbances. In actual clinical practice, within highly sterile hospital surgical environments, biological particles (Bacteria-Carrying Particles) released by medical staff constitute one of the primary contamination sources in operating rooms, potentially leading to surgical site infections in patients [25]. Second, the lack of modeling for equipment interference. The obstructive effects of obstacles such as surgical lights and instrument carts on airflow are often oversimplified; in complex layouts like integrated operating rooms, this can result in significant discrepancies between simulated airflow patterns and actual vortex distributions [26]. Third, the static assumption of boundary conditions: parameters such as air supply volume and pressure differentials are typically set as fixed values in simulations, failing to account for instantaneous fluctuations induced by actions like door openings. However, airflow disturbances during door openings can completely disrupt the positive pressure state of the operating room [27].

5.2. The Quantitative Balance Dilemma in Multi-objective Optimization

The operating room ventilation system must simultaneously achieve three key objectives: cleanliness, thermal comfort, and energy consumption control. However, a mature quantitative equilibrium framework that accounts for the interdependent relationships among these objectives has not yet been established. The application of multi-objective optimization algorithms remains in its infancy; although methods such as the Takauchi algorithm and the Grey Wolf Optimizer demonstrate potential for local parameter optimization, they lack a comprehensive optimization framework covering the entire system lifecycle, particularly a dynamic adaptation mechanism tailored to different surgical scenarios [28].

The differentiation among standard systems further complicates balance efforts. Requirements for air change rates vary by country by 20%-30%; for instance, ASHRAE Standard 170 specifies laminar supply air velocities of 0.25–0.35 m/s, whereas domestic standards mandate 0.2–0.3 m/s for localized unidirectional airflow systems. Such discrepancies undermine the consistency in establishing optimization benchmarks. Moreover, existing standards predominantly focus on static parameter limits without incorporating dynamic evaluation metrics for energy consumption and comfort, hindering the practical implementation of multi-objective optimization solutions.

5.3. Technical Gaps in Mass Transfer Control for Special Scenarios

The widespread adoption of minimally invasive surgeries has made aerosol pollution control a new safety challenge, as existing ventilation systems generally exhibit insufficient efficiency in capturing surgical smoke. Aerosols generated by devices such as high-frequency electrosurgical units and ultrasonic scalpels typically have particle sizes ranging from 0.1 to 5 μm, containing harmful substances like benzene and formaldehyde, as well as active pathogens. Particles with diameters less than 2.5 μm (PM2.5) are predominantly distributed in the near-ground atmospheric layer, posing a threat to human health. Prolonged exposure to PM2.5 pollution carries an extremely high risk of disease onset [29].

Current prevention and control technologies exhibit significant shortcomings: first, insufficient synergy between local exhaust systems and surgical procedures; second, imbalance in the coordination between ventilation airflow and smoke dispersion; third, inadequate specificity of filtration technologies.

6. Future Outlook

In recent years, the widespread adoption of technologies such as CFD, AI, and BIM has opened new avenues for system optimization; however, a significant gap remains between theoretical research and engineering practice. Identifying the minimum energy consumption required for creating clean operating rooms and addressing energy conservation and emission reduction challenges focus on the core pain points of operating room ventilation systems. By integrating technological trends, feasible solutions are proposed to provide references for industry research and application.

6.1. Technology Integration

Promote the integrated application of ANSYS CFD with BIM, digital twins, and AI. Single CFD simulations are insufficient to support airflow optimization and intelligent management throughout the entire lifecycle of operating rooms (design–construction–operation and maintenance). BIM technology, leveraging its advantages such as visual modeling, multi-disciplinary collaboration, and end-to-end information integration, effectively addresses issues in hospital buildings—including pipeline conflicts, low spatial utilization rates, and suboptimal operational efficiency—significantly enhancing project quality and management efficiency. During the operation phase, digital twins enable real-time monitoring of operating room parameters such as air velocity, temperature and humidity, cleanliness levels, and pressure differentials. Combined with Reduced Order Modeling (ROM) and reinforcement learning, this approach

facilitates rapid flow field prediction and intelligent ventilation system regulation, dynamically balancing infection control, thermal comfort, and energy efficiency objectives. Studies have demonstrated that BIM-CFD synergy can improve ventilation design efficiency in clean operating rooms by over 30%, while the integration of digital twins and CFD enables real-time alerts and dynamic adjustments, reducing surgical site infection risks [30].

6.2. Green and Energy-Saving

Demand-side dynamic regulation technology enables precise alignment between energy consumption and performance. This study analyzes energy-saving and consumption-reduction technologies for hospital cleanroom HVAC systems by examining aspects such as regional planning of operating room HVAC systems, HVAC system configuration, and automatic fresh air volume regulation. Key measures include rational design of the common HVAC system, separate installation of indoor and outdoor purification HVAC systems, upgrading secondary return air systems, implementing fresh air dehumidification, and adopting decentralized fresh air systems. Additionally, neural network models are employed to achieve automatic fresh air volume regulation, effectively reducing HVAC operational energy consumption while maintaining optimal temperature control and cleanliness levels [31].

6.3. Conclusion

The optimization of operating room ventilation systems has entered a transformation phase characterized by "precision, intelligence, and low carbon." Current research shortcomings in dynamic modeling, multi-objective balancing, and response to specialized scenarios fundamentally stem from insufficient integration of technologies and an incomplete evaluation framework. Future research on operating room airflow organization will focus on two major directions: first, promoting the integration of ANSYS CFD with BIM, digital twins, and AI to achieve comprehensive airflow optimization and intelligent regulation throughout the operating room's lifecycle, thereby enhancing design efficiency and reducing infection risks; second, adopting demand-side dynamic control technologies—such as zoned air conditioning configurations, secondary return air systems, and neural network-based fresh air regulation—to ensure cleanliness while achieving energy efficiency and environmental sustainability.

References

[1] Zhou Liya, Zhu Weifeng. Application of dynamic air purification and disinfection technology in hospital clean operating rooms [J]. Industrial Microbiology, 2024,54(06):37-39.

[2] Huang Jing, Cui Can, Zhou Shuli, et al. Feasibility study on the use of air particle counting method for evaluating operating room air quality [J]. China Journal of Disinfection, 2019,36 (04):250-252.

[3] Yan Jianmin, Li Jie, Yang Yongmei, et al. Design of an integrated operating room air conditioning system [J]. HVAC, 2020,50(01):97–102. DOI: 10.19991/j. hvac1971.2020.01.021.

[4] Li Xiaolei, Ni Ming. Research on standards for pharmaceutical cleanrooms and related controlled environments [J]. China Pharmaceutical Affairs, 2020,34(10):1165-1170. DOI: 10. 16153/ j.1002-7777.2020.10.007.

[5] Gao Qing, Liu Ringshuai. Construction and performance verification of a green, low-energy passive building exterior window system [J]. China Building Decoration & Renovation, 2025, (09):91-93. DOI: CNKI: SUN: ZJIA.0.2025-09-021.

[6] Haiyi Du, Juan Shi, Shengpeng Chen, Siyuan Cheng, Zhenqian Chen, Energy consumption of a novel floor radiant cooling system in large space buildings,Applied Thermal Engineering, Volume257,PartB,2024,124336,ISSN13594311,https://doi.org/10.1016/j.applthermaleng.2024.124336.

[7] Zhang Zechao. Analysis of the outdoor wind environment for an irregular building complex on a coastal campus [D]. Shandong Jianzhu University, 2023. DOI: 10.27273/d.cnki. gsajc. 2023.000633.

[8] Zhou Weiming. Research on Numerical Simulation and Optimization Design of Airflow Organization in Dual-Isolation Wards [D]. Jiangsu University of Science and Technology, 2024. DOI: 10.27171/d. cnki.ghdcc. 2024.000941.

[9] Bian Jinlong. Study on the dispersion patterns of human exhaled aerosols in tiered ventilation NPI wards [D]. Chongqing University of Science and Technology, 2023. DOI: 10.27854/d.cnki.gcqkj. 2023.000129.

[10] Guo F, [10] Guo F, et al. A full-scale experimental study of thermal environment in operating room considering surgical lamps and occupants. Building and Environment. 2022; 207: 108416.

[11] Ankang Kan, Jin Hu, Thermal performance evaluation on vacuum insulation panels in composite building envelope under large temperature variations, International Journal of Low-Carbon Technologies, Volume 12, Issue 1, March 2017, Pages 51–53, https://doi.org/10.1093/ijlct/ctv026

[12] Alamdari F, Alamdari F, et al. Thermal comfort in operating rooms: A review. Energy Procedia. 2017; 111: 164–173.

[13] Guo Peishan. Experimental and Simulation Study on Airflow Organization for Large-Scale Paroxysmal Dust Source Control [D]. Donghua University, 2008.

[14] EN ISO 14644-3:2019. Cleanrooms and associated controlled environments – Part 3: Test methods.

[15] Du Shiyuan, Xu Wenhua. Exploration of an Active Control Method for Pressure Differential and Air Volume in Clean Rooms [J]. Refrigeration Technology, 2007, (01):38–42. DOI: CNKI: SUN: ZLJS.0.2007-01-015.

[16] Cen Dongdong, Cao Shijie. Simulation of the impact of human movement on pollutant dispersion in cleanrooms based on the momentum source method [J]. Mechanical Design and Manufacturing Engineering, 2020,49(12):113–117. DOI: CNKI: SUN: JXZZ.0.2020-12-026.

[17] Liu Haiyang. Study on airflow disturbance and biological particle diffusion patterns in dynamic operating room environments [D]. North China Electric Power University, 2021. DOI: 10.27139/d.cnki.ghbdu. 2021.000241.

[18] Liu Shuanqiang, Liu Xiaohua, Jiang Yi. Application of independently controlled temperature and humidity air conditioning systems in hospital buildings [J]. HVAC, 2009,39(04):68-73.

[19] Yan Chang. Implementation of flow field visualization based on MATLAB and CFD databases [J]. Henan Science and Technology, 2019, (02):17–19.

[20] Yang Shaodong, Ding Changfu, Wang Yin, et al. Study on airflow characteristics in a nuclear facility building based on PIV experiments [J]. HVAC 2025,55(05):98–105+125. DOI: 10.19991/j.hvac1971.2025.05.13.

[21] Deng Zhiyao, Lin Yaolin, Liu Naiwei. Study on Room Load Using Different Partitioning Strategies in Regional Models

[J/OL]. Intelligent Computers and Applications, 1–17 [2026-04-17]. https://doi.org/10.20169/j.issn.2095-2163.24091401.

[22] Xue Puning. Research on Intelligent Operation Decision-Making Methods for Smart Heating Systems [D]. Harbin Institute of Technology, 2021. DOI: 10.27061/d.cnki.ghgdu. 2021.005261.

[23] Tian Yushi. Research and Application of Energy-Saving Technologies for Automated Electrical Equipment in Buildings [D]. Jilin Jianzhu University, 2015.

[24] Zhai Yuyang. Study on operating room-related factors and preventive measures for surgical site infections in surgical patients [J]. Chinese and Foreign Medical Journal, 2020,39(30): 51-53. DOI: 10.16662/j.cnki.1674-0742.2020.30.051.

[25] Yin D. Effects of human thermal plume on the diffusion of biological particles in hospital surgical microenvironments [D]. North China Electric Power University, 2022. DOI: 10. 27139/d.cnki. ghbdu. 2022.000653.

[26] Andrea Baldini, Kier Blevins, Daniel Del Gaizo, Oliver Enke, Karan Goswami, William Griffin, Pier Francesco Indelli, Toby Jennison, Eustathios Kenanidis, Paul Manner, Robin Patel, Teija Puhto, Parag Sancheti, Rahul Sharma, Rajeev Sharma, Rjajendra Shetty, Rami Sorial, Naasha Talati, T. David Tarity, Kevin Tetsworth, Christos Topalis, Eleftherios Tsiridis, Annette W-Dahl, Matthew Wilson,General Assembly, Prevention, Operating Room - Personnel: Proceedings of International Consensus on Orthopedic Infections,The Journal of Arthroplasty, Volume 34, Issue 2, Supplement,2019,Pages S97-S104,ISSN 0883-5403,https://doi.org/10. 1016/j.arth. 2018. 09.059.

[27] He Yanxia, Mo Meizhen, Zhang Xiaochun, et al. Effect of surgical room personnel flow control measures on changes in airborne bacterial counts [J]. Massage and Rehabilitation Medicine, 2020,11(23):87–89. DOI: 10.19787/j.issn.1008-1879. 2020.23.029.

[28] Lü Bo, Wang Ming, Yang Dongrun, et al. A three-layer optimization scheduling strategy for HVAC systems based on an improved hybrid algorithm [J/OL]. Computer Applications, 1–13 [2026-04-18]. https://link.cnki. net.urlid/51. 1307.TP. 20260413.1743.006.

[29] Zhang Taixin. Study on the hourly aerosol pollution distribution and its changes in typical urban agglomerations in Himawari-8 China [D]. Wuhan University, 2020. DOI: 10.27379/d.cnki.gwhdu. 2020.000775.

[30] Li Zan, Liu Quanjun, Xiong Zhengchao, et al. Research on the Application Progress of BIM Technology in the Full Life Cycle of Medical Complexes [C] // China Society for Graphic Design Architectural Information Modeling (BIM) Professional Committee, Beijing Urban Construction Group Co., Ltd. Proceedings of the 11th National BIM Academic Conference. Beijing Urban Construction Group Co., Ltd.; 2025:195–199. DOI: 10.26914/c.cnkihy.2025.066968.

[31] Zhao Lina, Sheng Zhiguo, Dong Ming. Analysis of Energy-Saving Measures for Hospital Clean Air Conditioning Systems [J]. Equipment Management and Maintenance, 2024, (12): 178–181. DOI: 10.16621/j.cnki.issn1001-0599.2024.06D.61.